

中国科学：信息科学

# SCIENCE CHINA

## Information Sciences

*Sponsored by*

CHINESE ACADEMY OF SCIENCES

NATIONAL NATURAL SCIENCE FOUNDATION OF CHINA

[info.scichina.com](http://info.scichina.com)

[www.springer.com/scp](http://www.springer.com/scp)

[www.springerlink.com](http://www.springerlink.com)

### Special Focus on Information Fusion

*Guest Editors:* JING ZhongLiang, LEUNG Henry, LI YuanXiang



## Honorary Editor General

### Editor General

### Editor-in-Chief

### Executive Associate Editor-in-Chief

**ZHOU GuangZhao** (Zhou Guang Zhao)

**ZHU ZuoYan** *Institute of Hydrobiology, CAS*

**LI Wei** *Beihang University*

**WANG DongMing** *Centre National de la Recherche Scientifique*

## Associate Editors-in-Chief

**GUO Lei** *Academy of Mathematics and Systems Science, CAS*

**HUANG Ru** *Peking University*

**QIN YuWen** *National Natural Science Foundation of China*

**SUN ZengQi** *Tsinghua University*

**YOU XiaoHu** *Southeast University*

**ZHAO QinPing** *Beihang University*

**ZHAO Wei** *University of Macau*

## Members

**CHEN JianEr**  
*Texas A&M University*

**DU Richard LiMin**  
*Voxeas Institute of Technology*

**GAO Wen**  
*Peking University*

**GE ShuZhi Sam**  
*National University of Singapore*

**GUO GuangCan**  
*University of Science and Technology of China*

**HAN WenBao**  
*PLA Information Engineering University*

**HE JiFeng**  
*East China Normal University*

**HU WeiWu**  
*Institute of Computing Technology, CAS*

**HU ZhanYi**  
*Institute of Automation, CAS*

**IDA Tetsuo**  
*University of Tsukuba*

**JI YueFeng**  
*Beijing University of Posts and Telecommunications*

**JIN Hai**  
*Huazhong University of Science and Technology*

**JIN YaQiu**  
*Fudan University*

**JING ZhongLiang**  
*Shanghai Jiao Tong University*

**LI Joshua LeWei**  
*University of Electronic Science and Technology of China*

**LIU DeRong**  
*Institute of Automation, CAS*

**LIN HuiMin**  
*Institute of Software, CAS*

**LIN ZongLi**  
*University of Virginia*

**LONG KePing**  
*University of Science and Technology Beijing*

**LU Jian**  
*Nanjing University*

**MEI Hong**  
*Peking University*

**MENG LuoMing**  
*Beijing University of Posts and Telecommunications*

**PENG LianMao**  
*Peking University*

**PENG QunSheng**  
*Zhejiang University*

**SHEN ChangXiang**  
*Computing Technology Institute of China Navy*

**SUN JiaGuang**  
*Tsinghua University*

**TANG ZhiMin**  
*Institute of Computing Technology, CAS*

**TIAN Jie**  
*Institute of Automation, CAS*

**TSAI WeiTek**  
*Arizona State University*

**WANG Ji**  
*National University of Defense Technology*

**WANG JiangZhou**  
*University of Kent*

**WANG Long**  
*Peking University*

**WU YiRong**  
*Institute of Electronics, CAS*

**XIE WeiXin**  
*Shenzhen University*

**XU Jun**  
*Tsinghua University*

**XU Ke**  
*Beihang University*

**YIN QinYe**  
*Xi'an Jiaotong University*

**YING MingSheng**  
*Tsinghua University*

**ZHA HongBin**  
*Peking University*

**ZHANG HuanGuo**  
*Wuhan University*

**ZHOU Dian**  
*The University of Texas at Dallas*

**ZHOU ZhiHua**  
*Nanjing University*

**ZHUANG YueTing**  
*Zhejiang University*

## Editorial Staff

**SONG Fei**

**FENG Jing**

**ZHAO DongXia**

**Special Focus on Information Fusion**

On the sensor order in sequential integrated probability data association filter.....	491
WANG Yang, JING ZhongLiang, HU ShiQiang, ZHANG HongJian & WU JingJing	
Joint spatial registration and multi-target tracking using an extended PM-CPHD filter.....	501
LIAN Feng, HAN ChongZhao, LIU WeiFeng, LIU Jing & YUAN XiangHui	
Globally optimal distributed Kalman filtering fusion.....	512
SHEN XiaoJing, LUO YingTing, ZHU YunMin & SONG EnBin	
Data fusion for target tracking in wireless sensor networks using quantized innovations and Kalman filtering.....	530
XU Jian, LI JianXun & XU Sheng	
Integrated optimization methods in multisensor decision and estimation fusion.....	545
LUO YingTing, SHEN XiaoJing & ZHU YunMin	
A new DSMT combination rule in open frame of discernment and its application.....	551
WEN ChengLin, XU XiaoBin, JIANG HaiNa & ZHOU Zhe	
Some notes on betting commitment distance in evidence theory.....	558
HAN DeQiang, DENG Yong, HAN ChongZhao & YANG Yi	
A dual-kernel-based tracking approach for visual target.....	566
ZHANG CanLong, JING ZhongLiang, JIN Bo & LI ZhiXin	
A multi-cue mean-shift target tracking approach based on fuzzified region dynamic image fusion.....	577
XIAO Gang, YUN Xiao & WU JianMin	
Fusion tracking in color and infrared images using joint sparse representation.....	590
LIU HuaPing & SUN FuChun	
Video motion stitching using trajectory and position similarities.....	600
CHEN XiaoWu, LI Qing, LI Xin & ZHAO QinPing	
Pan-sharpening: a fast variational fusion approach.....	615
ZHOU ZeMing, LI YuanXiang, SHI HanQing, MA Ning & SHEN Ji	
An algorithm for high precision attitude determination when using low precision sensors.....	626
CAO Lu, CHEN XiaoQian & SHENG Tao	

**RESEARCH PAPER**

Complexity of synthesis of composite service with correctness guarantee.....	638
DENG Ting, HUAI JinPeng & WO TianYu	
RST transforms resistant image watermarking based on centroid and sector-shaped partition.....	650
ZHAO Yao, NI RongRong & ZHU ZhenFeng	
CUDA-Zero: a framework for porting shared memory GPU applications to multi-GPUs.....	663
CHEN DeHao, CHEN WenGuang & ZHENG WeiMin	
A fast successive over-relaxation algorithm for force-directed network graph drawing.....	677
WANG YongXian & WANG ZhengHua	
Achieving fair service with a hybrid scheduling scheme for CICQ switches.....	689
HU HongChao, GUO YunFei, YI Peng & LAN JuLong	
Estimation of convergence rate for multi-regression learning algorithm.....	701
XU ZongBen, ZHANG YongQuan & CAO FeiLong	
The optimization of replica distribution in the unstructured overlays.....	714
FENG GuoFu, LI WenZhong, LU SangLu, CHEN DaoXu & BUYYA Rajkumar	
A new intelligent prediction system model-the compound pyramid model.....	723
YANG BingRu, QU Wu, WANG LiJun & ZHOU Ying	

# RST transforms resistant image watermarking based on centroid and sector-shaped partition

ZHAO Yao<sup>1,2\*</sup>, NI RongRong<sup>1,2\*</sup> & ZHU ZhenFeng<sup>1,2\*</sup>

<sup>1</sup>*Institute of Information Science, Beijing Jiaotong University, Beijing 100044, China;*

<sup>2</sup>*Beijing Key Laboratory of Advanced Information Science and Network Technology, Beijing 100044, China*

Received April 22, 2011; accepted July 7, 2011

**Abstract** A novel digital watermarking scheme featuring centroid-based sectoring is proposed in this paper. To get higher robustness against geometric attacks, such as rotation, scaling, and translation (RST), a delicate synchronization mechanism was developed and incorporated into the proposed approach. During the process of watermark embedding, the original image was partitioned into sectors based on the image centroid. Synchronization information as well as the message bits is then embedded into these sectors. With the help of the centroid-based sectoring and synchronization information, the proposed approach is capable of restoring the correct sectoring even if it has experienced severe geometric distortion. This attribute ensures the correct recovery of embedded watermarks and contributes to the robustness of the proposed scheme. A series of experiments have been conducted to verify the feasibility and effectiveness of the proposed approach. Experimental results show that the proposed scheme possesses good robustness against RST attacks and considerable robustness against other common image processing attacks.

**Keywords** digital watermarking, geometrical transform attacks, RST transforms

**Citation** Zhao Y, Ni R R, Zhu Z F. RST transforms resistant image watermarking based on centroid and sector-shaped partition. *Sci China Inf Sci*, 2012, 55: 650–662, doi: 10.1007/s11432-011-4470-x

## 1 Introduction

Digital watermarking techniques have been proposed to embed signatures in the multimedia data to identify the owner and the intended recipients, and to check the authenticity of the multimedia data. Applications include copyright protection, owner authentication, content authentication, tamper detection, data hiding and so on. Most watermarking schemes are designed to resist attacks from many signal and image processing operations including but not limited to compression and filtering [1–3]. However, recently it has become clear that even the smallest geometric distortion can prevent the detection of a watermark. This problem is most apparent when the original image is unavailable to the detector [4]. How to efficiently resist such kinds of attacks remains to be an unanswered question and thus a challenging direction to study in the area of watermarking research. Several different schemes have been proposed and will be subsequently discussed.

There are three main streams for watermarking schemes immune to geometric attacks, namely exhaustive search, geometrically reverse transformation, and geometric invariants. For the first category,

Corresponding author (email: yzhao@bjtu.edu.cn, rri@bjtu.edu.cn, zhgzhu@bjtu.edu.cn)

typical geometric transformations commonly used in image manipulation are applied on the whole image, and in general can be represented by certain mathematical formulations. One straightforward approach to identify the transformation is to perform an exhaustive detection considering all possible geometric transformations on the watermarked image. However, the computational cost could be dramatically high [2]. In the second category, geometrically reverse transformation and correlation are used to extract embedded watermarks. Pereira et al. proposed a resynchronization mechanism based on the template technology [5]. Another researcher, Kutter, proposed a similar method called self-reference method [6]. However, the method does not embed a special template; instead it repeatedly embeds the same watermark in four different positions and estimates the geometric transform by the 9 autocorrelation function (ACF) peaks of the predicted watermark. In the third category, geometric invariants are used to modulate the watermark signal [7]. In [8–10], watermark embedding was conducted in the RST invariant Fourier-Mellin domain. Similarly, Solachidis et al. [11] used a circularly symmetric watermark in the discrete Fourier transform (DFT) domain. Image salient feature points, known as invariant to geometric transforms, have also been used in watermarking [12–18]. In 1962, Hu introduced moment invariants which are position, size and orientation independent [19]. Alghoniemy et al. [20] first utilized geometric moment-based invariants to design a zero-bit watermark, which is robust against geometric manipulations and filtering, etc. Ping Dong et al. [21] proposed a multi-bit normalization based watermarking method. Recently Zernike moments are introduced into image watermarking [22–24].

Centroid, as a kind of moment, has been used in robust image watermarking in our earlier work [25], where three centroids of an image's three MSB bitplanes are used to segment the image into sectors and watermark bits are embedded into the sectors. However, when the embedding capacity is high or the three centroids are located too closely for some images, the extractor may fail to correctly synchronize the segmentation as in the embedding.

In this work, we will take the advantage of moments in the development of a watermarking scheme robust to RST transforms. The proposed scheme firstly calculates the centroid of the most significant bitplane (MSB) of the original image, and uniformly partitions the image into sectors based on the centroid. Then the scheme embeds synchronization bits and message bits into sectors using quantization index modulation (QIM). In detection, the scheme also partitions the watermarked image as for embedding. It is capable of restoring the correct partitioning even if the watermarked image is subject to RST transforms and other image processing. The proposed scheme makes use of the geometric invariant property of the centroid, synchronization and auto-oriented partitioning, and leads to good robustness and considerable capacity.

The remaining sections of the paper are organized as follows: Section 2 describes our proposed embedding process, followed by Section 3 which describes the extraction process. Some experimental results are presented in Section 4 and finally Section 5 concludes this paper.

## 2 Watermark embedding procedure

The embedding procedure is shown in Figure 1. An image  $I$  is inputted into the system of which the MSB bitplane centroid is calculated thereafter. After image  $I$  is partitioned and quantized, we receive the new watermarked image ( $I_W$ ).

### 2.1 Image partitioning

A gray scale image  $I$  consists of  $j$  number of bitplanes. For example, a 256-level image has  $j=8$  bitplanes, i.e. Bitplane 7, Bitplane 6, Bitplane 5, . . . , Bitplane 1, and Bitplane 0.

For the MSB plane, i.e. Bitplane 7, the centroid  $O : (x_0, y_0)$  is calculated as follows:

$$x_0 = \frac{m_{10}}{m_{00}}, y_0 = \frac{m_{01}}{m_{00}}, \quad (1)$$

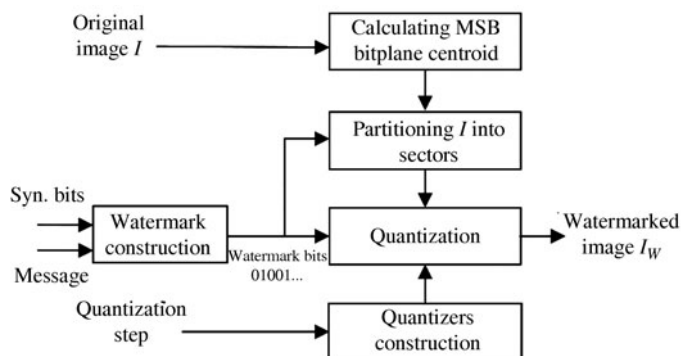


Figure 1 Schematic diagram of watermark embedding.

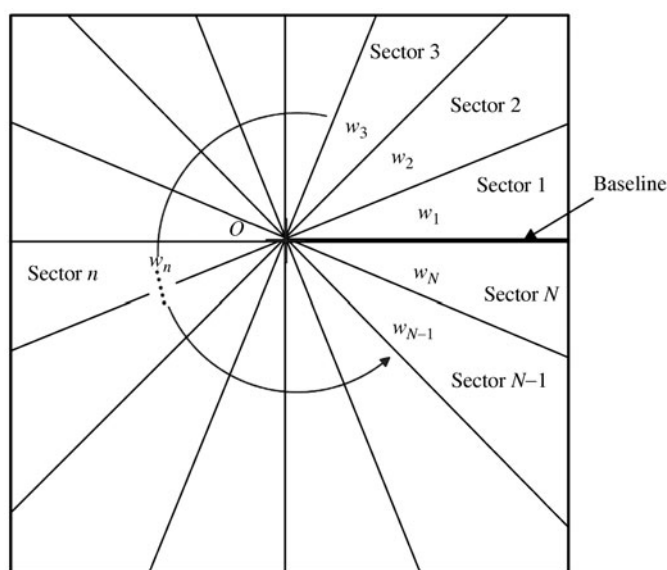


Figure 2 Partitioning an image into sectors based on the centroid.

where  $m_{00}$ ,  $m_{01}$  and  $m_{10}$  are Cartesian moments, given by

$$m_{pq} = \sum_{x=0}^{N_1-1} \sum_{y=0}^{N_2-1} x^p y^q B(x, y). \tag{2}$$

$B(x, y)$  is the bit value at position  $(x, y)$  of Bitplane 7, and  $N_1 \times N_2$  is the size of image  $I$ .

With the centroid  $O$  as origin and the horizon as the baseline, i.e. the thick line in Figure 2, we anti-clockwise uniformly segment the image into  $N$  sectors by central angle, where  $N$  is the total number of watermark bits. The procedure is shown in Figure 2. The sectors are called Sector 1, Sector 2, ..., Sector  $N$  in order.

The reason why we use the centroid of Bitplane 7 instead of the entire gray level is to easily maintain an unchanged centroid during watermark embedding. Subsection 2.3 will describe the details. Since the MSB of a pixel is least likely to be changed by the most signal processing operations [26], the centroid position of Bitplane 7 is also least likely to be changed by image processing and geometric transforms, as will be verified by the experimental results.

### 2.2 Watermark construction

The watermark  $w = w_1 w_2 \cdots w_n \cdots w_N = \underbrace{w_1 w_2 \cdots w_M}_{\text{syn. bits}} \underbrace{w_{M+1} w_{M+2} \cdots w_{M+L}}_{\text{message}}$ , where  $w_n \in \{0, 1\}$ ,  $N = M + L$  consists of two parts:  $M$ -bit synchronization bits  $w_1 w_2 \cdots w_M$  and  $L$ -bit message  $w_{M+1} w_{M+2} \cdots$

$w_{M+L}$ . Any message to be embedded can be represented as a bit sequence  $w_{M+1}w_{M+2} \cdots w_{M+L}$ . The synchronization bits and the message bits are concatenated together and form the watermark. The  $M$ -bit synchronization is a pseudo-random bit sequence which is generated using a secret key  $\mathbf{K}$  as a seed. The key, hence the synchronization bit sequence  $w_1w_2 \cdots w_M$ , is also known to watermark extractor. By pattern matching, the synchronization can be used for the watermark extractor to correctly locate the beginning of the message. The length  $M$  of synchronization is pre-selected which affects the matching accuracy, message capacity and false matching probability, while the message length  $L$  is determined by the message.

### 2.3 Quantization

Each watermark bit will be embedded anti-clockwise in each sector using QIM [27].

First, we construct two quantizers  $Q(\cdot; s)$ , where  $s \in \{0, 1\}$ . In this paper, we consider the case where  $Q(\cdot; s)$  is a uniform, scalar quantizer with stepsize  $\Delta$  and the quantizer ensemble consists of two quantizers shifted by  $\Delta/2$  with respect to each other.  $\Delta$  is pre-defined and known to both embedder and extractor; it affects both the robustness to common signal processing and the watermarked image quality. In order to further increase the robustness while ensuring the transparency, human visual system (HVS) can be considered in choosing the stepsize, so the stepsize should be different for images with different textures.

Image pixels are processed in raster order; that is, pixels are quantized serially, left-to-right for each image row, beginning with the top row. For any pixel  $I(x, y)$ , using the centroid as origin, its polar angle is calculated, and then we can easily determine which sector  $I(x, y)$  belongs to based on the polar angle. If  $I(x, y) \in \text{Sector } n$ , then it is quantized as  $I_W(x, y)$  with quantizer  $Q(\cdot; w_n)$ .

$$I_W(x, y) = Q(I(x, y); w_n). \tag{3}$$

In order to obtain the same centroid position as the original image in detection process, Bitplane 7 should remain unchanged after embedding. However, without any constraint, after the quantization, Bitplane 7 may be changed. Thus, we modify the quantization process of (3) to that of (4).

$$I_W(x, y) = \begin{cases} Q(I(x, y); w_n), & \text{if } Q(I(x, y); w_n) \geq I^7(x, y), \\ Q(I(x, y); w_n) + \Delta, & \text{if } Q(I(x, y); w_n) < I^7(x, y), \end{cases} \tag{4}$$

where  $I^7(x, y) = I(x, y) \&(10000000)_2$ .

Equation (4) ensures that the pixel has been quantized according to the watermark bit and that the MSB bitplane keeps unchanged.

After every pixel is quantized, the watermark embedding process is finished.

All the pixels in the original image will be quantized during the embedding, so the time exhausted are nearly the same no mater into how many sectors the original image is partitioned. The quantization operation in (4) is easy, so the embedding process is fast.

## 3 Watermark extraction procedure

The extracting process is shown as Figure 3.

In watermark extraction, the first three steps are the same as in embedding: calculate the image centroid, partition  $I_W$  into sectors and finally construct quantizers. Next we will introduce the other two steps in detail: finely tuning the partitioning and watermark extraction.

### 3.1 Finely tuning partitioning(FTP)

In order to correctly extract the watermark, it is quite vital to correctly partition the watermarked image. We wish to make such partition that during detection, it completely overlaps with that of the partitioning yielded from embedding. This is shown in Figure 4. In the figure, the dashed sectors are the old partitioning created in the embedding. After attacks, such as rotation, the baseline of the old parti-

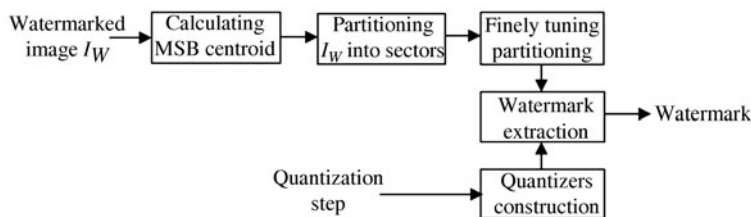


Figure 3 Schematic diagram of watermark extraction.

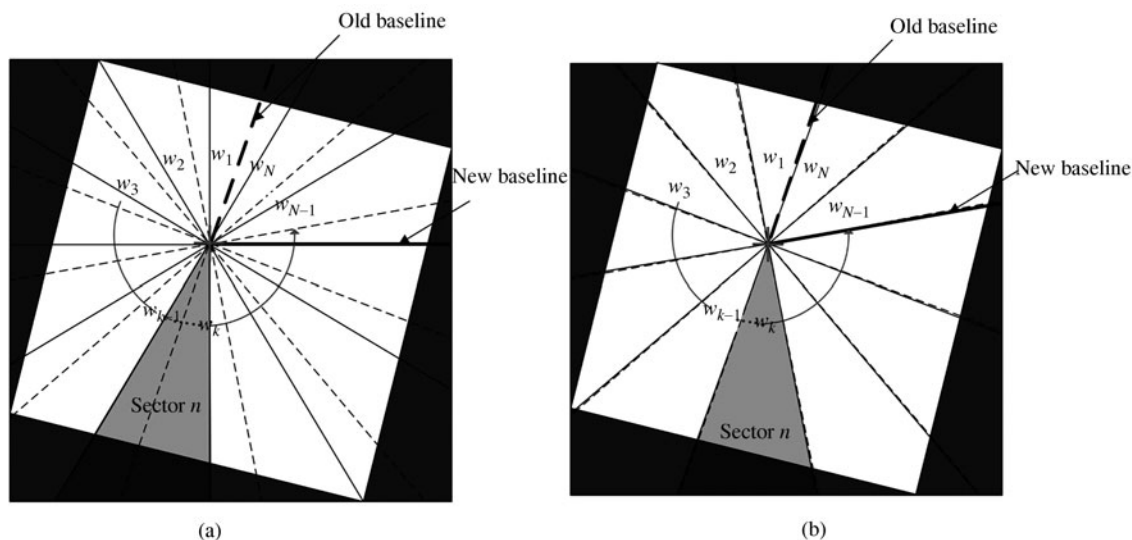


Figure 4 (a) The partitioning in detection (solid) usually does not overlap with the partitioning in embedding (dashed); (b) after finely tuning partitioning, the two partitionings nearly overlap together.

tioning, i.e. the dashed thick line in Figure 4(a) has been rotated to another position, and therefore the position of each sector may change. However, in the detection, the detector does not know what manipulations have been done; thus it can only partition the image from the new baseline, i.e., the horizon. The solid sectors in Figure 4(a) are the new partitioning. The two partitions typically do not completely overlap.

An automatic orienting/aligning procedure called FTP is proposed to solve this problem. The proposed procedure is capable of automatically rotating the new partitioning to the “correct” position, as shown in Figure 4(b); that is, after the correction, the sectors in the new partitioning should overlap with the old ones, even though the new baseline may not overlap with the old one.

It can be expected that a sector in the new partitioning of an attacked image will cover two adjacent sectors of the old partitioning, such as Sector  $n$  in the gray area of Figure 4(a). In some area of Sector  $n$ , the pixels are embedded with a watermark bit, for example,  $w_{k-1}$ ; the others are embedded with watermark bit  $w_k$ . If the pixel is detected to embed bit 1, then it is called “1” pixel; otherwise, it is called “0” pixel.

Let  $\text{Num}_n(1)$  denote the number of “1” pixels in Sector  $n$  and  $\text{Num}_n(0)$  denote the number of “0” pixels in Sector  $n$ . We define

$$\text{Maj}_n(\theta) = \begin{cases} \text{Num}_n(1), & \text{if } \text{Num}_n(1) \geq \text{Num}_n(0), \\ \text{Num}_n(0), & \text{otherwise,} \end{cases} \quad (5)$$

as the majority pixel number in Sector  $n$  when the new partitioning is rotated by an angle  $\theta$ . Figure 5 is used to clarify the concept. If  $w_{k-1} \neq w_k$ , it is obvious that the gray area with oblique in Figure 5(a) is the majority pixels. If we rotate the current partitioning by a central angle  $\theta$ , as shown in Figure 5(b), then the majority pixels area change, and thus  $\text{Maj}_n(\theta)$  changes. It is worthwhile to notice that as  $\theta$  increases,  $\text{Maj}_n(\theta)$  increases or decreases monotonously.

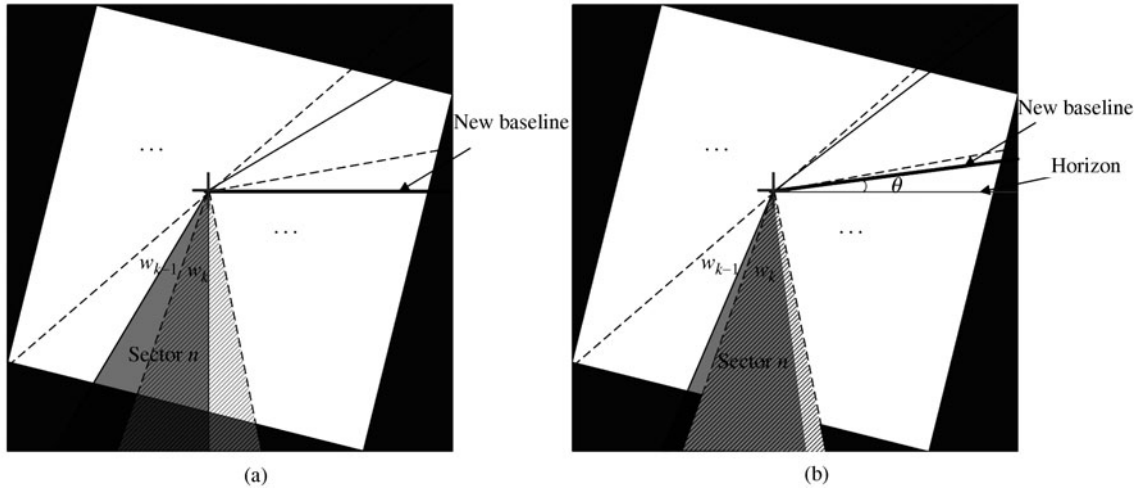


**Figure 5** The majority pixels in a sector. (a) Sector  $n$  in the initial partitioning; (b) sector  $n$  when new partitioning rotated by angle.

On the other hand, if  $w_{k-1} = w_k$ , the entire sector makes up the majority pixels area. As the partitioning rotate angle  $\theta$  changes, the  $\text{Maj}_n(\theta)$  does not change.

Define

$$\text{Maj}_{\text{all}}(\theta) = \sum_{n=1}^N \text{Maj}_n(\theta), \tag{6}$$

as the majority pixel number in the whole image when the partitioning is rotated by an angle  $\theta$ .

As  $\theta$  varies,  $\text{Maj}_n(\theta)$  of some sectors may change monotonously, and others remain the same. As a whole,  $\text{Maj}_{\text{all}}(\theta)$  will change monotonously. It is clear that only when the new partitioning is rotated to exactly overlap with the old partitioning as shown in Figure 4(b), does  $\text{Maj}_{\text{all}}(\theta)$  reach its maximum.

Using  $\text{Maj}_{\text{all}}(\theta)$  as the criteria, we are able to first determine which direction we need to rotate the partitioning, and secondly, how much we need to rotate it. The tuning process is shown in Figure 6.

In FTP, the watermark extractor first rotates the new baseline clockwise and anti-clockwise respectively at a tuning step  $\Delta_{\angle}$ , and then checks  $\text{Maj}_{\text{all}}(\theta)$  to determine in which direction we should remedy the partitioning. After that, the extractor increasingly rotates the partitioning until  $\text{Maj}_{\text{all}}(\theta)$  reaches the maximum.

From Figure 4 and the above analysis, we can conclude that the goal of FTP is to rotate the new baseline to its nearest old sector side, and therefore we can conclude that the maximum angle  $\theta_{\text{opt}}$  to be rotated satisfies

$$\theta_{\text{opt}} \leq \frac{\theta_{\text{Sector}}}{2}, \tag{7}$$

where  $\theta_{\text{Sector}}$  is sector angle. In all the experiments in the paper, the tuning step  $\Delta_{\angle} = \frac{\theta_{\text{Sector}}}{10}$ , so the extractor maximally needs 5 times searches to reach its optimal position. Alternatively we also use coarse to fine searching strategy; that is, at the coarse search period, we select a coarse tuning step, for example,  $\Delta_{\angle} = \frac{\theta_{\text{Sector}}}{6}$ . After reaching the best position, we use a fine tuning step, for example,  $\Delta_{\angle} = \frac{\theta_{\text{Sector}}}{12}$ , to finely search for the best position near the coarse best position. Thus we can quickly and accurately reach the best position. Deciding what bit is embedded in a pixel is actually a quantization process, which is easy to operate. In our experiments, a laptop computer with a duo Intel CPU at 2.4 GHz is used as the computing platform. All the processes are performed in MATLAB without any optimization. It averagely takes about 1 minute to finish watermark extraction for a  $512 \times 512$  image.

### 3.2 Watermark extraction

After the optimal angle  $\theta_{\text{opt}}$  is obtained, we extract the watermark bits with minimum distance decoder and then locate the synchronization to get the embedded message.

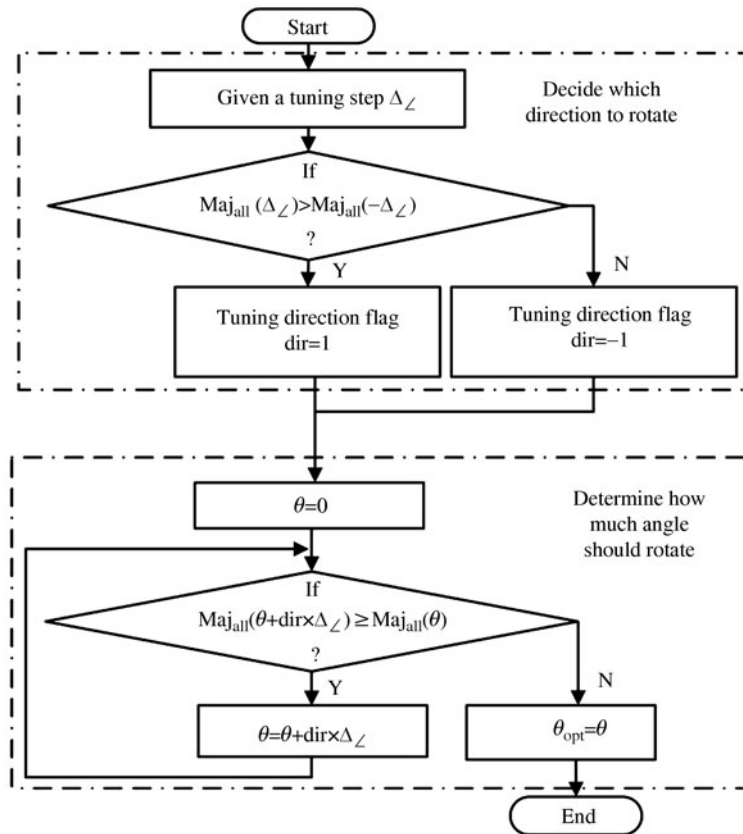


Figure 6 The steps of finely tuning process.

Every pixel  $I'_W(x, y)$  in Sector  $n$  is quantized with  $Q(\cdot; 0)$  and  $Q(\cdot; 1)$ , and the quantization errors  $d_n(I'_W(x, y), 0)$ ,  $d_n(I'_W(x, y), 1)$  are calculated.

$$d_n(I'_W(x, y), 0) = |I'_W(x, y) - Q(I'_W(x, y); 0)|, \tag{8}$$

$$d_n(I'_W(x, y), 1) = |I'_W(x, y) - Q(I'_W(x, y); 1)|. \tag{9}$$

Then the total square quantization errors for all the pixels in Sector  $n$  can be calculated as

$$d_n(0) = \sum_{(x,y) \in \text{Sector } n} d_n^2(I'_W(x, y), 0), \tag{10}$$

$$d_n(1) = \sum_{(x,y) \in \text{Sector } n} d_n^2(I'_W(x, y), 1). \tag{11}$$

According to  $d_n(0)$  and  $d_n(1)$ , we can determine the watermark bit  $w_n$  in Sector  $n$ .

$$w_n = \begin{cases} 1, & \text{if } d_n(0) > d_n(1), \\ 0, & \text{otherwise.} \end{cases} \tag{12}$$

After every watermark bit is extracted, we get a watermark bit sequence; however, for the moment, the bit sequence may be different from the original watermark bit sequence. If all the watermark bits are correctly extracted, the bit sequence should be the circle-shifted version of the original sequence. We then circle shift the extracted bit sequence bit by bit and compare the first  $M$  bits with the synchronization bits; if there is a match, we then locate the synchronization and subsequently get the message. In order to resist flip operation attack, we also reverse the order of the extracted sequence and locate the synchronization accordingly.

The synchronization bits embedded are very important for message extraction; however, after attacks or image processing, some synchronization bit errors may occur. Therefore, in our scheme, during each

possible  $M$  bits to  $M$  bits comparison, if there are more than or equal to  $M - O$  bits matchable, we call it a match, where  $O$  is a pre-selected parameter.

There are possible multiple positions for the matching of the synchronization bits between the extracted and embedded watermarks. We next derive the probability that multiple matches occur.

Under the rule of bit sequence match defined above, for an  $M$ -bit synchronization, the probability of not matching with another  $M$ -bit sequence is given by

$$P = 1 - \left( \sum_{i=0}^O \binom{M}{i} \right) \cdot \frac{1}{2^M}. \quad (13)$$

In the extracted  $N$ -bit sequence and its reverse ordered sequence, except the correct match position, there are totally  $2N - 1$  possible positions to compare the synchronization, so the probability that multiple matches occur can be given by

$$\begin{aligned} P_{MM} &= P(\text{any match } 2N - 1 \text{ possible positions}) \\ &= 1 - P(\text{no match at any } 2N - 1 \text{ positions}) \\ &= 1 - \left( 1 - \left( \sum_{i=0}^O \binom{M}{i} \right) \cdot \frac{1}{2^M} \right)^{2N-1}. \end{aligned} \quad (14)$$

For example, if  $M=20$ ,  $N=120$  and  $O=2$ , then  $P_{MM} = 4.70 \times 10^{-2}$ .

If multiple synchronization matches occur, we choose the match with the most matching bits, or the first match when matching bits are equal, to locate the start of the message.

## 4 Experimental results

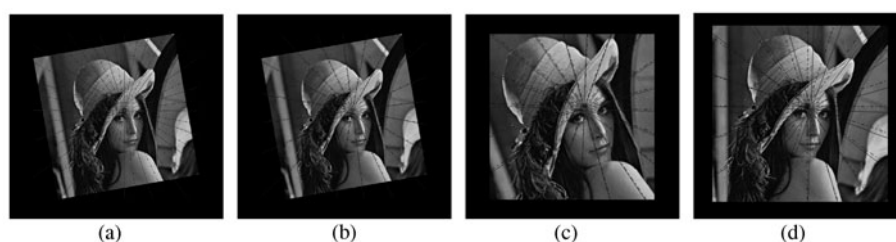
A series of experiments was conducted to verify the feasibility and effectiveness of the proposed approach. In our scheme, it is critical for the extractor to be re-synchronized in order to extract the embedded message correctly. In the proposed scheme, the re-synchronization relies mainly on two mechanisms: the centroid and the sectoring. The centroid should be nearly constant and the reconstructed sector partition should be correct.

Figure 7 shows the centroid locations of the  $512 \times 512$  standard image Lena under some typical image processing. To amplify the minor differences, only the part near the centroid is displayed, where the cross in the images represents the centroid position. Also the distances between the centroid locations of the attacked watermarked images and the original image are calculated. The distance is calculated as follows: First, calculate the centroid location of the attacked watermarked image, second, geometrically reverse transform the centroid position, and then calculate the position distance between the centroid and the original image centroid. In Figure 7(k)–(o), the watermarked image is rotated by a certain angle, then cropped and returns the central portion which is of the same size as the original. In Figure 7(p)–(t), the watermarked image is translated by some pixels. If the new coordinates are outside the image, the translate operator will normally ignore them, and involved black margins are cropped away. All the interpolation operations involved in rotations and scaling transforms of this paper are bilinear interpolation. Obviously the centroids in Figure 7(a)–(k) except Figure 7(g) stay nearly in the same position. It implies that the centroid is a very robust invariant under manipulations of this kind. The image in Figure 7(g) has been seriously blurred by Gaussian noise, so the centroid moves several pixels away from the original. In Figure 7(l)–(t), since parts of the rotated images are cropped, the centroids in these situations may drift away. In these situations, if the images are cropped too much, it will bring about negative impact on the subsequent partitioning. However, in practice, the images will not be cropped too much, or the malicious manipulations are trivially known.

Figure 8 shows the performance of FTP. The watermarked Lena is rotated or translated. In the detection, without finely tuning, the partitioning does not overlap with the original, as shown in Figure 8(a). If we use the proposed method to finely tune the partitioning, the two partitions nearly overlap

Centroid location							
Centroid bias	0	0	0.7225	0.3913	0	0.7420	5.4546
	(a)	(b)	(c)	(d)	(e)	(f)	(g)
Centroid location							
Centroid bias	0.7697	0.4714	1.5085	1.4311	4.3517	7.0209	13.3704
	(h)	(i)	(j)	(k)	(l)	(m)	(n)
Centroid location							
Centroid bias	12.5719	4.0193	7.7276	11.1876	14.4708	17.3684	
	(o)	(p)	(q)	(r)	(s)	(t)	

**Figure 7** The centroid locations of Lena under some typical image processing. (a)Original image:  $512 \times 512$  Lena; (b) watermarked Lena; (c) watermarked Lena rotated by 20 degrees; (d) watermarked Lena scaled by 1.5 times; (e) watermarked Lena translated by  $20 \times 20$  pixels; (f) watermarked Lena attacked by Gaussian noise  $N(0,0.001)$ ; (g) watermarked Lena attacked by Gaussian noise  $N(0,0.005)$ ; (h) watermarked Lena compressed by JPEG with quality factor 75; (i) watermarked Lena compressed by JPEG with quality factor 50; (j) watermarked Lena lowpass filtered by average with  $3 \times 3$  windows; (k) watermarked Lena rotated by 1 degree with cropping; (l) watermarked Lena rotated by 5 degrees with cropping; (m) watermarked Lena rotated by 10 degrees with cropping; (n) watermarked Lena rotated by 20 degrees with cropping; (o) watermarked Lena rotated by 45 degrees with cropping; (p) watermarked Lena translated by  $5 \times 5$  pixels with cropping; (q) watermarked Lena translated by  $10 \times 10$  pixels with cropping; (r) watermarked Lena translated by  $15 \times 15$  pixels with cropping; (s) watermarked Lena translated by  $20 \times 20$  pixels with cropping; (t) watermarked Lena translated by  $25 \times 25$  pixels with cropping.



**Figure 8** Performance of finely tuning partitioning. In the experiment, the dash lines indicate the original partition in embedding; the solid lines indicate the partition in the extraction process. (a) Rotated by 20 degrees without finely tuning; (b) rotated by 20 degrees with finely tuning; (c) rotated by 20 degrees plus cropping with finely tuning; (d) translated by  $[20,20]$  plus cropping with finely tuning.

together, as shown in Figure 8(b). Figure 8(c) also gives the finely tuning effect when the watermarked image is rotated and cropped; the performance is nearly identical with that of Figure 8(b). Figure 8(d) shows the finely tuning effect when the watermarked image is translated and cropped. Since the centroid had drifted away considerably, the performance is not as good as in Figure8(b) and Figure8(c). Nevertheless, finely tuning can still find out the best orientation.

We now turn our attention to the performance of watermark extraction.

Five standard  $512 \times 512$  images, including Airplane, Boat, House, Elaine and Lena, are used as test images. In all the tests,  $M = 20$ , and the capacity or message capacity mentioned below means the bits length for the message, i.e.  $L$ , excluding the synchronization. Without using any attack, we can embed and successfully extract a message of 2500 bits without any error, where  $\Delta=6$ , and the average peak signal-to-noise ratio (PSNR)=43.23 dB.

We then examine the performance of our scheme under RST attacks. Bit error rate (BER) is used as the criterion and defined as the percentage of bits that have errors relative to the total number of message bits. In all the experiments here,  $\Delta=6$ . Figure 9(a) shows the curves of BER versus message capacity  $L$ , when the watermarked image is rotated by 5 degrees. When the capacity is low, for example, less than 350 bits, the scheme can successfully resist the rotation attack without any errors. As the capacity increases, the BER is increased. There exists a transition period when the BER varies from 0 to steady 0.5. In the transition period, there are fluctuations in the BER that means at some point, the BER is small, and at some point, the BER is large. In this period, due to the high capacity, error in the bit extraction of each sector may occur and thus the extracted synchronization may contain errors, and so the matching of the synchronization is sometimes correct and sometimes wrong. If the synchronization is correctly located, then the message can then be correctly located, and so the BER is low. If the synchronization is not correctly located, then the message is wrongly located, and the BER reaches almost 0.5. Figure 9(b) displays the curves of BER versus message capacity  $L$ , when the watermarked image is rotated by 5 degrees with centrally cropping to its original size. The average PSNR is 43.13 dB. Figure 9(c) shows the curves of BER versus scaling manipulations, where  $L=200$  bits. We also investigate the performance against translation with cropping, as shown in Figure 9(d), where  $L=50$  bits. The scheme can achieve 0 bit error rate under  $[7, 7]$  translation plus cropping. Different images may have different performances mainly due to their different complexity. Usually, images with complex textures, such as Lena, may have lower performance, since when geometric transformations are applied, pixel interpolations will be used, and thus the pixel values will be changed. For complicated images, the pixel values are changed a lot; thus more QIM extraction errors will occur.

Robustness tests against JPEG compression and white Gaussian noise are also included in our experiments. Figure 10 reports the experimental results. In the experiment,  $L=200$  bits,  $\Delta=6$ , 10 and average PSNR= 43.22 dB, 39.53 dB respectively. Comparing the curves, we find that the larger  $\Delta$  is, the better the robustness. Figures 10(c) and (d) summarize the performance when the watermarked image is attacked by a white Gaussian noise. The white Gaussian noise is zero mean with different variance. It is evident that the quantization step affects the robustness and we have the same conclusion that the larger  $\Delta$  is, the better the robustness.

We also compare our proposed method with some other geometric robust method, i.e. Ping Dong's normalization method [21]. In [21], a geometric robust watermarking scheme based on image normalization is proposed, in which both watermark embedding and extraction are carried out with respect to an image normalized to meet a set of predefined moment criteria. Ten standard  $512 \times 512$  images, including Airplane, Boat, House, Peppers, Splash, Baboon, Couple, Lena, Elaine and Lake, are used as test images. In order to make comparison with [21], two capacities message, i.e. 50 bits and 100 bits plus 20-bit synchronization are embedded in the images using the proposed method, where  $\Delta=10$ , the average PSNR=38.7 dB. Then the watermarked images are distorted by a variety of geometric attacks to be listed in details below, BER is used as the criteria for comparison here.

Table 1 lists the comparing results.

The following is a list of attacks used to distort the images in the experiments [21].

1) Line and column removal: (a) (1, 1), (b) (1, 5), (c) (5, 1), (d) (5, 17), and (e) (17, 5), where each pair of numbers indicate the number of columns and rows removed, respectively. The removed columns/rows were equidistant.

2) Scaling by different factors: (a) 0.5, (b) 0.75, (c) 0.9, (d) 1.1, (e) 1.5, and (f) 2.

3) Rotation with different angles: (a)  $-15^\circ$ , (b)  $-5^\circ$ , (c)  $5^\circ$ , (d)  $25^\circ$ , (e)  $35^\circ$ , (f)  $45^\circ$ , and (g)  $80^\circ$ .

4) Shearing: (a) (0, 1%), (b) (0, 5%), (c) (1%, 0), (d) (5%, 0), (e) (1%, 1%) and (f) (5%, 5%), where

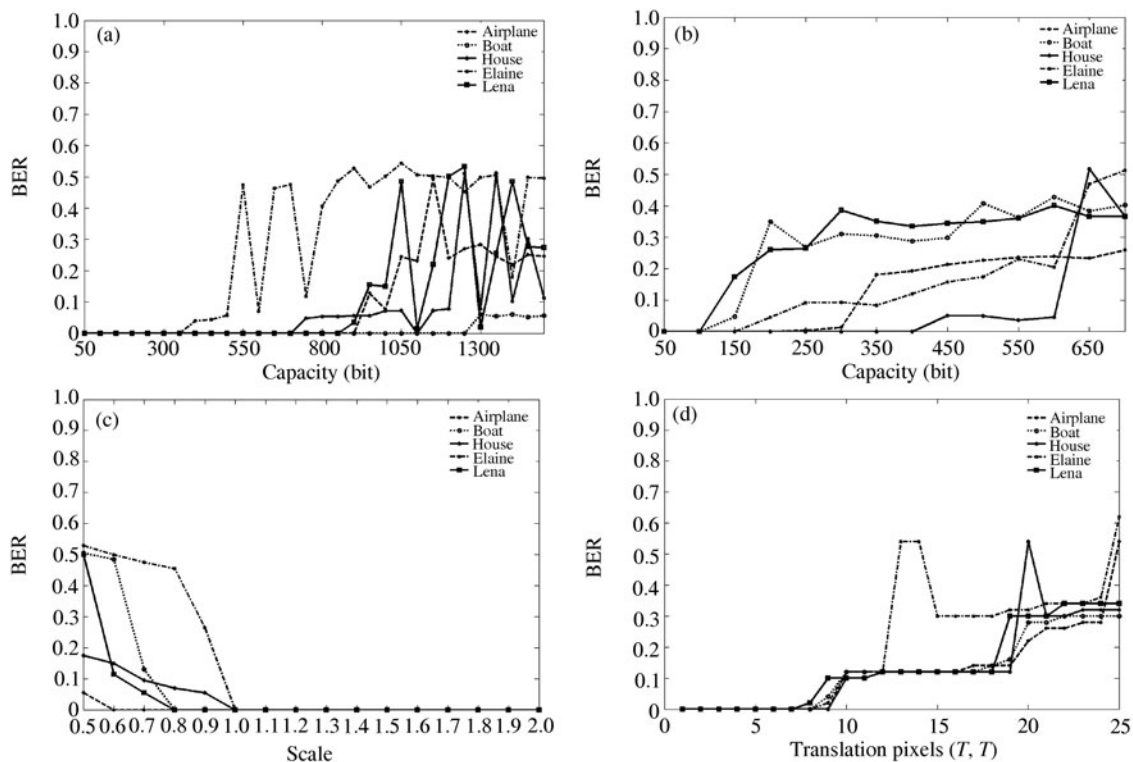


**Figure 9** (a) BER vs. capacity  $L$ , when rotated 5 degrees; (b) BER vs. capacity  $L$ , when rotated 5 degrees with cropping; (c) BER vs. scale where  $L=200$  bit; (d) BER vs. translation+cropping, where  $L=50$  bit.

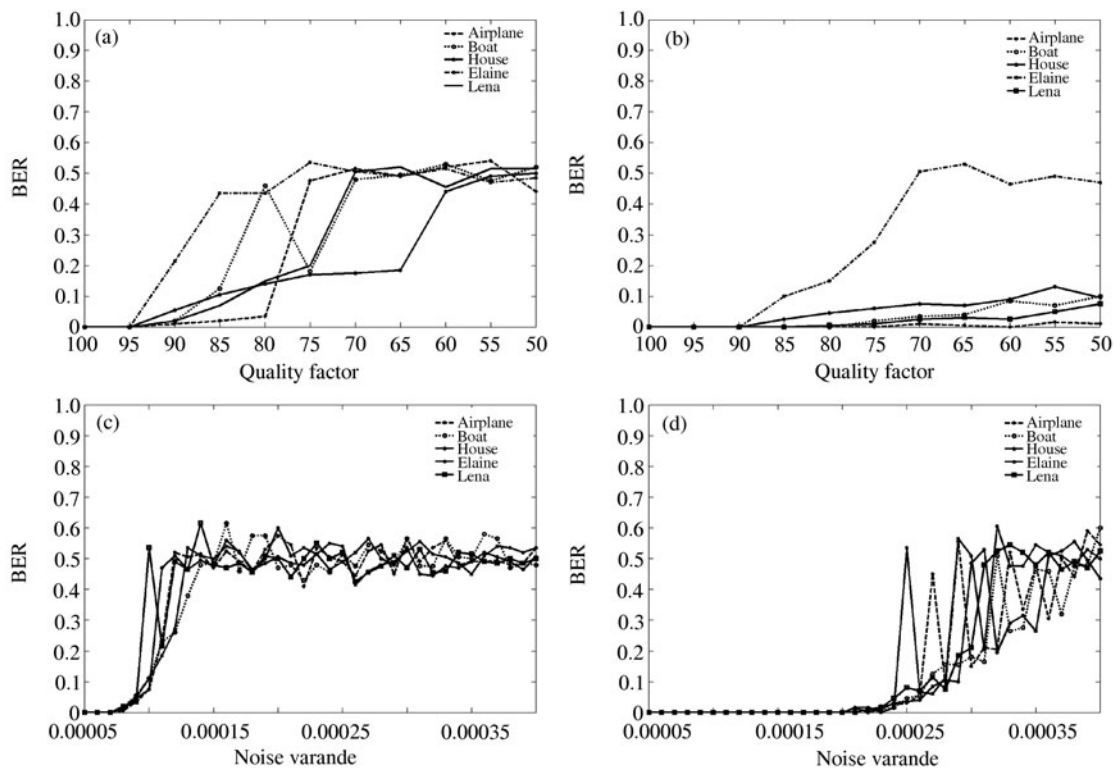


**Figure 10** Robustness against JPEG compression and white Gaussian noise. (a) BER vs. quality factor, where  $\Delta=6$ ; (b) BER vs. quality factor, where  $\Delta=10$ ; (c) BER vs. the variance of white Gaussian noise, where  $\Delta=6$ ; (d) BER vs. the variance of white Gaussian noise, where  $\Delta=10$ .

**Table 1** Performance comparison

Attacks/Cases	Removal	Scaling	Rotating	Shearing	Flip	RBA
a	M1	0	0	0	0	0.506
	M2	0	0.1040	0	0	0.0924
	M3	0	0.174	0	0	0.1924
b	M1	0.004	0	0	0	N/A
	M2	0	0	0	0	N/A
	M3	0	0.0508	0	0	N/A
c	M1	0	0	0	N/A	N/A
	M2	0	0	0	N/A	N/A
	M3	0	0.0133	0	0	N/A
d	M1	0.004	0	0	N/A	N/A
	M2	0	0	0	N/A	N/A
	M3	0	0	0	N/A	N/A
e	M1	0	0	0	0.002	N/A
	M2	0	0	0	0	N/A
	M3	0	0	0	0.0229	N/A
f	M1	N/A	0.048	0	0	N/A
	M2	N/A	0	0	0.1220	N/A
	M3	N/A	0	0	0.1343	N/A
g	M1	N/A	N/A	0	0	N/A
	M2	N/A	N/A	0	0	N/A
	M3	N/A	N/A	0	0	N/A

M1: Method in [21], Capacity=50.

M2: Proposed method, Capacity=50.

M3: Proposed method, Capacity=100.

each pair of numbers indicates the amount of shearing in the horizontal and vertical directions, respectively.

5) Horizontal and vertical flipping: (a) horizontal and (b) vertical.

6) StirMark random bending attack (RBA) [28].

From Table 1, we can see that when embedding the same payload, i.e. 50 bits, as in [21], our method can achieve better performance; when embedding with 100 bits, our method can still achieve comparable results.

## 5 Conclusions

A new digital watermarking scheme, distinguished with its robustness against geometric attacks, is developed and presented in this paper. Featuring centroid-based sectoring and synchronization bits, the proposed approach exploits geometric invariants for the modulation of watermark message. As a result, with the proposed approach, embedded watermarks will have better chance to survive under rotation, scaling, translation, and other image processing attacks. A series of experiments was conducted to verify the feasibility and effectiveness of the proposed approach. Experimental results reveal that the proposed scheme outperforms existing approaches in both capacity and robustness.

## Acknowledgements

This work was supported in part by National Basic Research Program of China (Grant No. 2011CB302204), National Science Foundation of China (Grant No. 61025013), Sino-Singapore JRP (Grant No. 2010DFA11010), Beijing Natural Science Foundation (Grant No. 4112043), and Fundamental Research Funds for the Central Universities (Grant No. 2009JBZ006-3). Special thanks go to Dr. Feng Wu of Microsoft Research Asia, Prof.

Jeng-Shyang Pan and Dr. Chin-Shiuh Shieh of Kaohsiung University of Applied Sciences, Taiwan and Kenneth Byrd, MSEE of Howard University, USA for their kind help.

## References

- 1 Tanaka K, Nakamura Y, Matsui K. Embedding secret information into dithered multilevel image. In: Proceedings of IEEE Military Communications Conference. CA: IEEE, 1990. 216–220
- 2 Langelaar G C, Setyawan I, Lagendijk R L. Watermarking digital image and video data: a state-of-the-art overview. *IEEE Signal Proc Mag*, 2000, 17: 20–46
- 3 Zeng W, Liu B. A statistical watermark detection technique without using original images for resolving rightful ownerships of digital images. *IEEE Trans Image Process*, 1999, 8: 1534–1548
- 4 Petitcolas F A P, Anderson R J, Kuhn M G. Attacks on copyright marking systems. In: Proceedings of Workshop Information Hiding. Portland: Springer-Verlag, 1998. 15–17
- 5 Pereira S, Ruanaidh J, Deguillaume F, et al. Template based recovery of fourier-based watermarks using log-polar and log-Log maps. In: Proceedings of IEEE International Conference on Multimedia Computing and Systems (ICMCS99). Florence: IEEE, 1999. 870–874
- 6 Kutter M. Watermarking resisting to translation, rotation and scaling. In: Proceedings of SPIE International Symposium on Voice, Video, and Data Communication. Boston: Society of Photo Optical, 1998. 423–431
- 7 Zhao Y, Lagendijk R L. Video watermarking scheme resistant to geometric attacks. In: Proceedings of IEEE International conference on image processing(ICIP2002). USA: IEEE, 2002. 22–25
- 8 Oruanaidh J, Pun T. Rotation, scale and translation invariant spread spectrum digital image watermarking. *Signal Process*, 1998, 66: 303–317
- 9 Lin C Y, Wu M, Bloom J A, et al. Rotation, scale, and translation resilient watermarking for images. *IEEE Trans Image Process*, 2001, 10: 767–782
- 10 Zheng D, Zhao J, Saddik A El. RST-invariant digital image watermarking based on log-polar mapping and phase correlation. *IEEE Trans Circ Syst Vid*, 2003, 13: 753–765
- 11 Solachidis V, Pitas I. Circularly symmetric watermark embedding in 2-D DFT domain. *IEEE Trans Image Process*, 2001, 10: 1741–1753
- 12 Inoue H, Miyazaki A, Yamamoto A, et al. A digital watermark technique based on the wavelet transform and its robustness on image compression and transformation. *IEICE Trans Fund Electr*, 1999, E82-A: 2–10
- 13 Bas P, Chassery J-M, Macq B. Geometrically invariant watermarking using feature points. *IEEE Trans Image Process*, 2002, 11: 1014–1028
- 14 Qi X, Qi J. Image content-based geometric transformation resistant watermarking approach. In: Proceedings of IEEE International Conference on Acoustics, Speech, and Signal Processing(ICASSP2005). Philadelphia: IEEE, 2005. 829–832
- 15 Qi X, Qi J. A robust content-based digital image watermarking scheme. *Signal Process*, 2007, 87: 1264–1280
- 16 Tang C W, Hang H M. A feature-based robust digital image watermarking scheme. *IEEE Trans Signal Process*, 2003, 51: 950–959
- 17 Cox I J, Kilian J, Leighton T, et al. Secure spread spectrum watermarking for multimedia. *IEEE Trans Image Process*, 1997, 6: 1673–1687
- 18 Davoine F, Bas P, Hebert P-A, et al. Watermarking et resistance aux deformations geometriques. In: Proceedings of Compression et Representation des Signaux Audiovisuels. France, 1999
- 19 Hu M-K. Visual pattern recognition by moment invariants. *IRE Trans Inform Theory*, 1962, IT-8: 179–187
- 20 Alghoniemy M, Tewfik A H. Geometric invariance in image watermarking. *IEEE Trans Image Process*, 2004, 13: 145–153
- 21 Dong P, Brankov J G, Galatsanos N P, et al. Digital watermarking robust to geometric distortions. *IEEE Trans Image Process*, 2005, 14: 2140–2150
- 22 Farzam M, Shirani S. A robust multimedia watermarking technique using Zernike transform. In: Proceedings of IEEE International Workshop Multimedia Signal Processing. France: IEEE, 2001. 529–534
- 23 Kim H S, Lee H K. Invariant image watermark using Zernike moments. *IEEE Trans Circ Syst Vid*, 2003, 13: 766–775
- 24 Xin Y, Liao S, Pawlak M. Circularly orthogonal moments for geometrically robust image watermarking. *Pattern Recogn*, 2007, 40: 3740–3752
- 25 Zhao Y, Pan J-S, Zhu Z F. RST resilient multi-bit image watermarking based on bitplane centroids. *Imaging Sci J*, 2008, 56: 41–48
- 26 Awrangjeb M, Murshed M. Robust signature-based geometric invariant copyright protection. In: Proceedings of IEEE International Conference on Image Processing (ICIP2006). USA: IEEE, 2006. 1961–1964
- 27 Chen B, Wornell G W. Preprocessed and postprocessed quantization index modulation methods for digital watermarking. In: Proceedings of SPIE: Security and Watermarking of Multimedia Contents II. San Jose: SPIE, 2000. 48–59
- 28 Petitcolas F A P. StirMark 3.1. <http://www.cl.cam.ac.uk/fapp2/watermarking/stirmark/>. 1999

## Information for authors

*SCIENCE CHINA Information Sciences (Sci China Inf Sci)*, cosponsored by the Chinese Academy of Sciences and the National Natural Science Foundation of China, and published by Science China Press, is committed to publishing high-quality, original results of both basic and applied research in all areas of information sciences, including computer science and technology; systems science, control science and engineering (published in Issues 1, 3, 5, 7, 9, 11); information and communication engineering; electronic science and technology (published in Issues 2, 4, 6, 8, 10, 12).

*Sci China Inf Sci* is published monthly in both print and electronic forms. It is indexed by Science Citation Index, Current Contents, Computer and Information Systems Abstracts, Corrosion Abstracts, Electronics and Communications Abstracts, Engineered Materials Abstracts, CompuMath Citation Index, Solid State and Superconductivity Abstracts, Mathematical Reviews, CSA Mechan. Transport. Engineer. Abstracts, MathSciNet, Aluminum Industry Abstracts, BioEngineering Abstracts.

Papers published in *Sci China Inf Sci* include:

**REVIEW** (20 printed pages on average) surveys representative results and important advances on well-identified topics, with analyses and insightful views on the states of the art and highlights on future research directions.

**RESEARCH PAPER** (no more than 15 printed pages) presents new and original results and significant developments in all areas of information sciences for broad readership.

**BRIEF REPORT** (no more than 4 printed pages) describes key ideas, methodologies, and results of latest developments in a timely manner.

Authors are recommended to use *Science China's* online submission services. To submit a manuscript, please go to [www.scichina.com](http://www.scichina.com), create an account to log in **JoMaSy** (Journal Management System), and follow the instructions there to upload text and image/table files.

Authors are encouraged to submit such accompanying materials as short statements on the research background and area/subareas and significance of the work, and brief introductions to the first and corresponding authors including their mailing addresses with post codes, telephone numbers, fax numbers, and e-mail addresses. Authors may also suggest several qualified experts (with full names, affiliations, phone numbers, fax numbers, and e-mail addresses) as referees, and/or request the exclusion of some specific individuals from potential referees.

All submissions will be reviewed by referees selected by the editorial board. The decision of acceptance or rejection of a manuscript is made by the editorial board based on the referees' reports. The entire review process may take 90 to 120 days, and the editorial office will inform the author of the decision as soon as the process is completed. If the editorial board fails to make a decision within 120 days, please contact the editorial office.

Authors should guarantee that their submitted manuscript has not been published before and has not been submitted elsewhere for print or electronic publication consideration. Submission of a manuscript is taken to imply that all the named authors are aware that they are listed as coauthors, and they have agreed on the submitted version of the paper. No change in the order of listed authors can be made without an agreement signed by all the authors.

Once a manuscript is accepted, the authors should send a copyright transfer form signed by all authors to Science China Press. Authors of one published paper will be presented one sample copy. If more sample copies or offprints are required, please contact the managing editor and pay the extra fee. The

full text opens free to domestic readers at [www.scichina.com](http://www.scichina.com), and is available to overseas readers at [www.springerlink.com](http://www.springerlink.com).

## Subscription information

**ISSN print edition:** 1674-733X

**ISSN electronic edition:** 1869-1919

Volume 55 (12 issues) will appear in 2012

### Subscription rates

For information on subscription rates please contact:

Customer Service

**China:** [sales@scichina.org](mailto:sales@scichina.org)

**North and South America:**

[journals-ny@springer.com](mailto:journals-ny@springer.com)

**Outside North and South America:**

[subscriptions@springer.com](mailto:subscriptions@springer.com)

### Orders and inquiries:

#### China

Science China Press

16 Donghuangchenggen North Street, Beijing 100717, China

Tel: +86 10 64015683

Fax: +86 10 64016350

Email: [informatics@scichina.org](mailto:informatics@scichina.org)

#### North and South America

Springer New York, Inc.

Journal Fulfillment, P.O. Box 2485

Secaucus, NJ 07096 USA

Tel: 1-800-SPRINGER or 1-201-348-4033

Fax: 1-201-348-4505

Email: [journals-ny@springer.com](mailto:journals-ny@springer.com)

#### Outside North and South America:

Springer Distribution Center

Customer Service Journals

Haberstr. 7, 69126 Heidelberg, Germany

Tel: +49-6221-345-0, Fax: +49-6221-345-4229

Email: [subscriptions@springer.com](mailto:subscriptions@springer.com)

**Cancellations** must be received by September 30 to take effect at the end of the same year.

**Changes of address:** Allow for six weeks for all changes to become effective. All communications should include both old and new addresses (with postal codes) and should be accompanied by a mailing label from a recent issue. According to § 4 Sect. 3 of the German Postal Services Data Protection Regulations, if a subscriber's address changes, the German Federal Post Office can inform the publisher of the new address even if the subscriber has not submitted a formal application for mail to be forwarded. Subscribers not in agreement with this procedure may send a written complaint to Customer Service Journals, Karin Tiks, within 14 days of publication of this issue.

**Microform editions** are available from: ProQuest. Further information available at <http://www.il.proquest.com/uni>

### Electronic edition

An electronic version is available at [springerlink.com](http://springerlink.com).

### Production

Science China Press

16 Donghuangchenggen North Street, Beijing 100717, China

Tel: +86 10 64015683 or +86 10 64034134

Fax: +86 10 64016350

Printed in the People's Republic of China

### Jointly published by

Science China Press and Springer

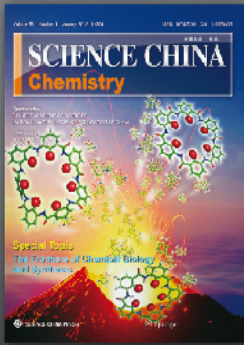
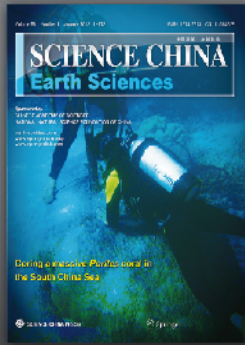


## SCIENCE CHINA Series | Chinese Science Bulletin

SCIENCE CHINA Series and the Chinese Science Bulletin are academic journals supervised by the Chinese Academy of Sciences, co-sponsored by the Chinese Academy of Sciences and the National Natural Science Foundation of China, jointly published by Science China Press and Springer. SCIENCE CHINA Series and the Chinese Science Bulletin have presented the finest examples of China's development in both natural sciences and technological research to the international scientific community. In order to fully express China's achievements in fundamental scientific and engineering research, SCIENCE CHINA Series is published in seven journals, i.e., Mathematics, Chemistry, Life Sciences, Earth Sciences, Technological Sciences, Information Sciences, and Physics (including Mechanics and Astronomy), with the Chinese Science Bulletin serving as a multidisciplinary journal.

- Peer-reviewed
- Indexed by SCI, CA, EI, etc.
- Online submission
- Easy access to the electronic version

Honorary Editor General: ZHOU Guangzhao (Zhou Guang Zhao) | Editor General: ZHU Zuoyan

Mathematics	Chemistry	Life Sciences	Earth Sciences
 <p>Monthly Editor-in-Chief YANG Le (YANG Lo)</p>	 <p>Monthly Editor-in-Chief LI LeMin</p>	 <p>Monthly Editor-in-Chief WANG DaCheng</p>	 <p>Monthly Editor-in-Chief SUN Shu</p>
Technological Sciences	Information Sciences	Physics, Mechanics & Astronomy	Chinese Science Bulletin
 <p>Monthly Editor-in-Chief YAN LuGuang</p>	 <p>Monthly Editor-in-Chief LI Wei</p>	 <p>Monthly Editor-in-Chief WANG DingSheng</p>	 <p>Published three times every month Editor-in-Chief XIA JianBai</p>

[www.scichina.com](http://www.scichina.com) | [www.springer.com/scp](http://www.springer.com/scp)

Sponsored by  
Chinese Academy of Sciences (CAS)  
National Natural Science Foundation of China (NSFC)

Published by  
Science China Press & Springer

ISSN 1674-733X



9 771674 733129

0 3>